Water Research 101 (2016) 127–136

Contents lists available at ScienceDirect

Water Research

journal homepage: www.elsevier.com/locate/watres

Characteristics of meso-particles formed in coagulation process causing irreversible membrane fouling in the coagulation-microfiltration water treatment

Q. Ding [a], H. Yamamura [a, *], N. Murata [b], N. Aoki [c], H. Yonekawa [d], A. Hafuka [a], Y. Watanabe [e]

[a] Faculty of Science and Engineering, Chuo University, 1-13-27 Kasuga, Bunkyo-ku, Tokyo 112-8551, Japan
[b] R&D Center, METAWATER Co., Ltd, 1 Maegata-cho, Handa, Aichi 475-0825, Japan
[c] Business Strategy Division, METAWATER Co., Ltd, JR Kanda Manseibashi Bldg, 1-25, Kanda-sudacho, Chiyoda-ku, Tokyo 101-0041, Japan
[d] Drinking Water Treatment Engineering Department, METAWATER Co., Ltd, 2-56 Suda-cho, Mizuho, Nagoya 467-8530, Japan
[e] Research and Development Initiatives, Chuo University, 1-13-27 Kasuga, Bunkyo-ku, Tokyo 112-8551, Japan

ARTICLE INFO

Article history:
Received 3 March 2016
Received in revised form
19 May 2016
Accepted 24 May 2016
Available online 26 May 2016

Keywords:
Coagulation-microfiltration
Irreversible membrane fouling
Meso-particles
Particle number
Zeta potential

ABSTRACT

In coagulation-membrane filtration water treatment processes, it is still difficult to determine the optimal coagulation condition to minimize irreversible membrane fouling. In microfiltration (MF), meso-particles (i.e., 20 nm–0.5 μm) are thought to play an important role in irreversible membrane fouling, especially their characteristics of particle number (PN) and zeta potential (ZP). In this study, a new nanoparticle tracker combined a high-output violet laser with a microscope was developed to identify the physicochemical characteristics of these microscopic and widely dispersed meso-particles. The effects of pH and coagulant dose on ZP and PN of micro-particles (i.e., >0.5 μm) and meso-particles were investigated, and then coagulation-MF tests were conducted. As the result, irreversible membrane fouling was best controlled for both types of membranes, while meso-particle ZP approached zero at around pH 5.5 for both types of natural water. Since PN was greatest under these conditions, ZP is more important in determining the extent of irreversible membrane fouling than PN. However, the acidic condition to neutralize meso-particles is not suitable for actual operation, as considering residual aluminum concentration, pipe corrosion, and chlorination efficiency. It is therefore necessary to investigate coagulants or other methods for the appropriate modification of meso-particle characteristics.

1. Introduction

Low-pressure membrane filtration methods facilitate simpler and more precise solid-liquid separation than sand filtration, and their introduction is therefore being considered at many water treatment plants. When introducing membrane filtration to water treatment processes, it is common to combine it with a preliminary coagulation process to remove dissolved organic matter and control membrane fouling (Gao et al., 2011; Huang et al., 2009; Matilainen et al., 2010; Singer, 1994). Also, because existing sand filter tanks can effectively be used as membrane submersion tanks, processing in which pre-coagulation and membrane filtration are combined is more often used in full-scale water treatment plants (as opposed to laboratories) than are ozone or activated carbon methods (Lebeau et al., 1998). However, although coagulation-membrane filtration processes are being considered as replacements for conventional water treatment processes, there are as yet no clear guidelines for optimal operation procedures when coagulation and membrane filtration are combined.

With sand filtration methods, it is important to optimize conditions such that turbidity and organic concentration are controlled. Optimal pH and coagulant dose are determined using jar tests. In most cases circumneutral conditions with a large dose of coagulants are used, to form large flocs (Amirtharajah and Mills, 1982). With membrane filtration methods, on the other hand, there is no need to sediment the flocs; instead they need only be larger than the membrane pore size. Thus these methods are more efficient than sand filtration because of the lower dose of coagulant

* Corresponding author.
E-mail address: yamamura.10x@g.chuo-u.ac.jp (H. Yamamura).

http://dx.doi.org/10.1016/j.watres.2016.05.076

required and smaller amount of coagulant sludge produced (Choi and Dempsey, 2004). In addition, floc formation and sedimentation basins are not required, so the size of processing facilities can be greatly reduced (Lebeau et al., 1998). A range of factors affect the process of membrane filtration and should be optimized, including the rate of removal of organic matter, turbidity, and the rate of membrane fouling. However, the conditions under which membrane fouling is best controlled differ from the optimal coagulation conditions obtained by jar tests (Choi and Dempsey, 2004; Kimura et al., 2008; Lee et al., 2000). In fact, optimal conditions are currently identified through a process of trial and error, by conducting membrane filtration tests under various coagulation conditions over an extended period of time. In order for the membrane filtration process to become more widespread, a method to replace the jar test that can simply and accurately explore the optimal coagulation conditions for pre-coagulation processing is crucial.

There are two types of membrane fouling: reversible and irreversible (Kimura et al., 2004). In reversible membrane fouling, there is a correlation between the fractal dimension of coagulation particles of 0.5 μm or greater (hereafter, micro-particles) and the rate of fouling. The mechanism that has been proposed to explain this is that floc strength increases with fractal dimension, and that any trans-membrane pressure (TMP) increase is thus inhibited by the formation of a coarse cake layer (Cho et al., 2005). It is however difficult to explain irreversible membrane fouling based on micro-particle behavior. This process is instead thought to be the result of microscopic particles with a particle size of 0.5 μm or less, which are close to or smaller than the membrane pore size (hereafter, meso-particles). Wiesner et al. (1989) calculated the balance between back-transportation speed and advection for each particle size, and proposed that particles around 0.1 μm in size are particularly likely to adhere to the membrane and are thus the primary culprits in membrane fouling. Furthermore, because physicochemical interactions between particles and the membrane surface are heavily involved in irreversible membrane fouling, we believe that in addition to rheological properties, physicochemical behaviors such as the effects of electrostatic force are instrumental in understanding the fouling mechanism of meso-particles.

Dynamic light scattering (DLS), light scattering, atomic force microscopes, and scanning electron microscopes have all been used in the investigation of the physicochemical behavior of microscopic particles (Buffle et al., 1998; Lead et al., 2006; Li et al., 1997; Perret et al., 1991; Tombacz et al., 1999). Because residual post-coagulation meso-particles are highly dispersed and therefore scatter light weakly, it is however extremely difficult to observe their particle characteristics underwater. Even with DLS, which is used in nano-particle characterization studies, the lower concentration limit for measurement is around 10 mg/L, and residual post-coagulation meso-particles, at a concentration of around 10,000 particles/mL, cannot be observed (Table S1). We have successfully detected, for the first time and with high sensitivity, underwater particles between 20 nm and 0.5 μm in size, by combining high-output short-wavelength laser light with an optical microscope, thus facilitating the measurement of zeta potential (ZP) and particle number (PN, lower bound 50,000 particles/mL) of meso-particles that remain after coagulation.

The purpose of this study was to describe the physicochemical behavior of meso-particles, which has to date been difficult to ascertain, and to identify the particular characteristics that affect irreversible membrane fouling. Meso-particles were operationally defined in this study as particles between 20 nm and 0.5 μm after fractionation of coagulated water, described in 2.2. Jar tests in detail. Using a polyaluminum chloride (PACl) with a basicity of 54.5% as coagulant, we varied the coagulation pH and PACl dose, measured the ZP and PN of the particles generated at coagulation, and compared the values for micro-particles and meso-particles. We also selected six sets of conditions from among the coagulation conditions tested, to conduct coagulation-MF tests using ceramic membranes and polyvinylidene fluoride (PVDF) membranes. This allowed us to identify the meso-particle characteristics that affect the rate of irreversible membrane fouling, and therefore propose a method for determining optimal coagulation conditions, based on meso-particle characteristics.

2. Materials and methods

2.1. Water samples and membranes

Water sampled from two representative bodies of surface water used as sources of drinking water in Japan (water A and water B) were used as raw water. Four hundred liters of water A and nine hundred liters of water B were collected, and large particles were removed using a 10 μm stainless steel cartridge filter. The characteristics of the two types of water are listed in Table 1. Water A was from a river which is about 59.5 km long and drains an area of 200 km^2. The level of organic matter in water A was very low compared to water B, as the total organic carbon (TOC) of water A was approximately one fourth of that of water B in Table 1. Water B was sampled from a water path running from a eutrophic lake. This lake's catchment area is approximately 220 km^2, which has recently been polluted by human sewage and agricultural fertilization. In addition, Table 1 showed that specific ultraviolet absorbance (SUVA) of water B was smaller than that of water A, which implies that water B contained much more hydrophilic organic matters including biopolymers (Kimura et al., 2014; Yamamura et al., 2014). We used two kinds of membranes for the filtration experiments: PVDF hollow fiber membrane (Asahi Kasei Chemicals, Japan) and ceramic monolith membrane (METAWATER, Japan). The nominal pore size of both membranes was 0.1 μm. For the PVDF membrane, 39 cm^2 of tiny-scale membrane modules were assembled with 10 fibers, each 10 cm in length. For the ceramic membrane, 53 of 55 holes in the 10 cm piece were filled with glue, leaving two holes with a combined surface area of 11 cm^2. The PVDF membrane used outside-in filtering and the ceramic membrane used inside-out filtering. Pure water permeability was determined for every module before it was used in the filtration experiments. ZP and PN of particles were examined through a series of jar tests under various pH and PACl doses.

2.2. Jar tests

The jar tests were performed at room temperature (18 ± 3 °C) using six standard 1 L beakers and a six-paddle jar test apparatus. We used PACl (10% as Al_2O_3) as the coagulant, at five different doses (0.3, 0.6, 1.0, 2.0 and 3.0 mg Al/L) with water A, and six doses (0.3, 0.6, 1.0, 2.0, 3.0 and 5.0 mg Al/L) with water B. We adjusted pH by adding 0.1 N sodium hydroxide or hydrochloric acid prior to the addition of PACl. The pH levels after PACl addition were 5.0, 5.5, 6.0, 6.5, 7.0, and 8.0. Mixing time was set at 3 min at 160 rpm (G

Table 1
Characteristics of the two types of surface water used in the tests.

	Water A	Water B
pH	7.9	8.0
TOC (Total organic carbon) (mg C/L)	1.1	4.3
UV_{254} (Ultraviolet absorbance at 254 nm) (cm^{-1})	0.023	0.080
SUVA (UV_{254}/TOC × 100) (L mg^{-1} m^{-1})	2.1	1.9
Turbidity (mg/L)	1.9	7.3
Alkalinity (mg $CaCO_3$/L)	9.9	70

value = 207 s^{-1}) for all samples, after which the coagulated water was allowed to settle for 3 min. In this study, we operationally define particles larger than 0.5 μm as micro-particles. After settling, the supernatant from 2 cm below the surface, equal to 200 mL, was collected. This fraction contained both micro-particles and particles smaller than 0.5 μm. Because large particles such as micro-particles will scatter the laser light if they are contained in the sample, this study eliminated such large particles and enable the lighting of smaller ones. The 200 mL sample was then centrifuged (3000 rpm, 10 min) and filtered using 1.0 and 0.5 μm membranes. This removed the micro-particles, so that the treated solution contained only particles smaller than 0.5 μm. As there is a possibility that some particles smaller than 0.5 μm might also be removed via centrifugation process, here we operationally define the residual particles between 20 nm and 0.5 μm in size as meso-particles. The PN and ZP of the micro-particles in the supernatant and meso-particles in the filtrate after filtration through the 0.5 μm membrane were determined separately. Dissolved organic carbon (DOC) and ultraviolet absorbance at 254 nm (UV_{254}) were also determined.

2.3. Coagulation-membrane filtration experiment

A schematic diagram of the coagulation-membrane filtration apparatus is shown in Figure S1. The six experimental conditions for each of the bench-scale experiments are summarized in Table 2, based on pH and PACl dose. We also conducted membrane filtration of raw water. Water A was filtered through the PVDF membrane after coagulation, and water B through both the PVDF and ceramic membranes. The PACl and raw water (after pH adjustment) were delivered to the mixing tank by two peristaltic pumps (Masterflex No.7523-90, Germany) at a constant flow rate, and were mixed at 160 rpm (GT = 37,260). The coagulation overflow ran directly into the filtration tank combined with submerged PVDF membrane module, simulating in-line coagulation (Li et al., 2011). The coagulated water from the PVDF membrane filtration tank was pumped to the ceramic membrane module by a peristaltic pump at a constant flow rate. Details of the mixing tank are summarized in Table 3.

The PVDF membrane was operated with a flux of 1.5 $m^3/m^2/d$, which was monitored using both a digital flow meter and manual analysis with a measuring cylinder. While water A was being filtered, hydraulic backwashing was conducted at a flux of 2.25 $m^3/m^2/d$ for 30 s every 15 min. While water B was filtered, hydraulic backwashing was conducted at a flux of 2.25 $m^3/m^2/d$ for 4 min every 30 min. During the last 3 s of each backwashing, about one third of the water combined with the settled sludge in the filtration tank was drawn out (recovery rate = 97%). For water A the filtration was conducted for 13 h, and for water B it was conducted for 120 h or until the TMP reached maximum operating pressure (60 kPa). During the coagulation of water B in the ceramic membrane filtration experiment, the flux was fixed at 4 $m^3/m^2/d$, which was monitored using a digital flow meter, and hydraulic backwashing (0.5 MPa) was conducted for 1.5 s every hour. The filtration was conducted for 120 h or until the TMP reached maximum operating pressure (100 kPa). The rate of fouling was monitored by recording TMP.

Table 2
Pre-coagulation conditions in the bench-scale coagulation-membrane filtration experiments.

Run no.	Water A		Water B	
	pH	PACl dose (mg Al/L)	pH	PACl dose (mg Al/L)
1	5.5	1.0	5.0	1.0
2	6.5	1.0	6.0	1.0
3	7.5	1.0	7.0	1.0
4	5.5	3.0	5.0	5.0
5	6.5	3.0	6.0	5.0
6	7.5	3.0	7.0	5.0

Table 3
Coagulation conditions in the mixing tank.

Condition	Water A	Water B
Mixing volume	100 mL	50 mL
Mixing speed	160 rpm	160 rpm
GT value	37,260	37,260
Raw water flow rate	22.9 mL/min	16.2 mL/min

2.4. Analytical methods

TOC and DOC were measured using a TOC analyzer (TOC-L; Shimadzu, Japan) and UV_{254} was measured with a UV spectrophotometer (UV-1800; Shimadzu). Residual aluminum was measured using an inductively coupled plasma-optical emission spectrometry analyzer (iCAP 7000; Thermo Fisher Scientific, USA). ZP was determined with a ZEECOM (ZC-3000 Series; Microtec, Japan). The ZEECOM was equipped with a violet laser (wave length: 405 nm, electric power: 65 mW) in addition to the microscope, and was specially manufactured for this study. In the cell channel of the ZEECOM there are two stagnant boundary layers. After determining the velocity of particles at both layers at voltages of 10–30 V, electrophoretic mobility U could be calculated using the equation $U = \nu/(V/L)$ (where ν is particle velocity (cm/s), V is voltage (V), and L is the distance between the electrodes (cm)). ZP could then be derived from the Smoluchowski equation: $\zeta = 4\pi\eta/\varepsilon \times U \times 300 \times 300 \times 1000$ (where ζ is ZP (mV), η is viscosity of water (g cm^{-1} s^{-1}), and ε is the relative permittivity of water (dimensionless)). As the distance observed by microscope was calibrated by measuring standard particles and time was always synced with computer, the velocity calculated from the distance and time could be guaranteed. The ZP value we used was the average of the ZP values at the two stagnant boundary layers after 50–200 measurements. We used the ZEECOM's scattered light mode when measuring the ZP of the particles in the supernatant, and thus measured only the average ZP of the micro-particles, as meso-particles cannot be detected by scattered light. We used the ZEECOM's violet laser mode when measuring the ZP of the meso-particles in the filtrates following filtration through the 0.5 μm membrane. The PN of the meso-particles was counted with the software WinROOF 2013 using the pictures obtained in the ZP measurement of the meso-particles. One picture is equivalent of 0.62 mm × 0.47 mm × 0.08 mm in volume, and therefore the counts were converted into volumetric concentrations by multiplying 43,240 to the counted meso-particles. The method applied for meso-particle count was got certified by the counting of known particles determined by Coulter counter (Multisizer 4e; Beckman Coulter, USA). The PN of the micro-particles was directly counted using a Hybrid Particle Counter (MW-SK121; METAWATER).

3. Results and discussion

3.1. Effects of coagulation conditions on the particle number

The effects of coagulation conditions (i.e., coagulation pH and PACl dose) on the PN of micro- and meso-particles in the two types of waters are shown in Fig. 1. Without PACl addition, PN of micro-particles and meso-particles in water A were about 7.0 × 10^5 and 6.0 × 10^6 particles/mL, both of which decreased when PACl was added (Fig. 1 (a, b)). For both of water, PN of micro-particles

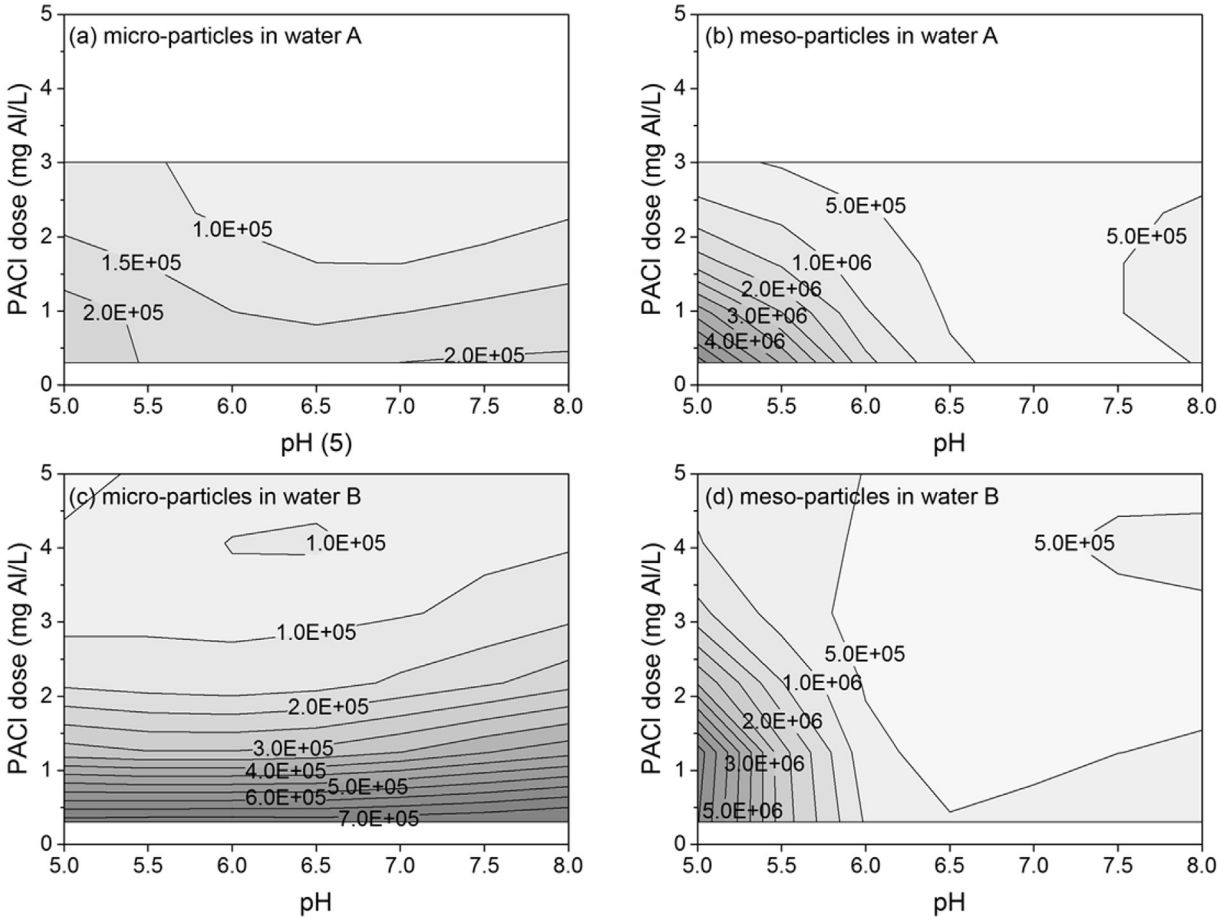

Fig. 1. Effects of pH and PACl dose during coagulation on particle numbers of: (a) micro-particles in water A; (b) meso-particles in water A; (c) micro-particles in water B; and (d) meso-particles in water B.

decreased with an increase in PACl dose, but less affected by pH (Fig. 1 (a, c)). The decrease in PN was particularly dramatic for doses of 2.0 mg Al/L and below. For water A (Fig. 1 (a)), at same PACl dose, minimum PN was seen at pH 6.5–7.0. This could be explained by conventional coagulation theory that cross-linking effect would be strongest around pH 7.0, at which condition particles would aggregate into larger ones thus lead to decrease of PN. However, for water B (Fig. 1 (c)), pH seems to have little effect on PN of micro-particles. The reason could be explained by comparing water qualities in Table 1. From Table 1, the lower value of SUVA of water B indicates that water B consisted more hydrophilic substances including biopolymers than water A, whose electric charge densities are close to zero (Buffle et al., 1998), which would be removed based on the mechanism that coprecipitation with coagulants rather than charge neutralization.

Since meso-particles have a different size distribution than micro-particles, we predicted that their physicochemical characteristics would differ greatly. PN of meso-particles were more strongly affected by coagulation pH than by the PACl dose (Fig. 1 (b, d)). PN increased with decreasing pH, and for both source waters reached a maximum at pH 5.0. We hypothesize that this was due to elimination of the Al polymer cross-linking effect caused by the form of the aluminum changing from a polymer to dissolved Al^{3+} (Duan and Gregory, 2003). PN of micro-particles were minimized at pH 6.5–7.0, but above pH 7.0 increased once again. We hypothesize that this is because aluminum hydroxide became the main component at high pH levels, so the formation of coarse flocs was inhibited (Duan and Gregory, 2003).

3.2. Effects of coagulation conditions on zeta potential

Floc charge plays an important role in the coagulation process. We therefore suggest that the differences between meso-particles and micro-particles in terms of PN, discussed above, may have been related to differences in zeta potential (Fig. 2).

The particle size distribution of meso-particles have been studied occasionally (Kimura et al., 2008; Stoller, 2009), but nothing has been reported regarding the charge of meso-particles. From Fig. 2 it is clear that the ZP characteristics of meso-particles and micro-particles differ. Under the same PACl dose, the neutralization point (ZP = 0) of meso-particles is at a lower pH than that of micro-particles. Thus while micro-particles are neutralized within a normal coagulation pH range (pH 6.0–7.0), meso-particles are not neutralized and left with a residual negative charge. In addition, the ZP of micro-particles increases linearly with PACl dose, but there is little change in the ZP of meso-particles, and even when a dose over 3.0 mg Al/L is added, the ZP cannot be neutralized at pH 6.0 and above. The similar trend was seen when using artificial water (Fig. 3).

Possible reasons for the neutralization point of meso-particles occurring at a lower pH than that of micro-particles are that: (1) the positive charge of the PACl increases as pH decreases; or (2) the

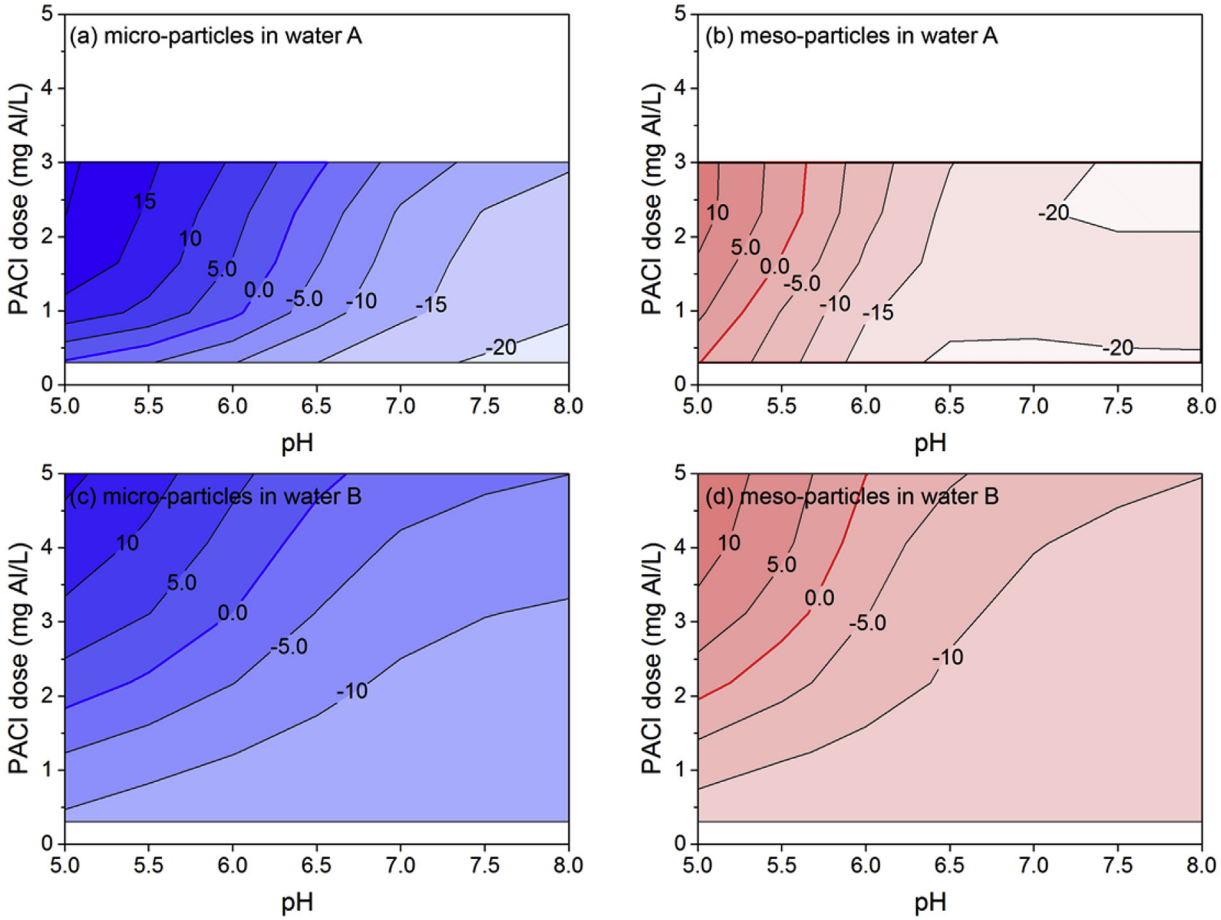

Fig. 2. Effects of pH and PACl dose during coagulation on the zeta potential of: (a) micro-particles in water A; (b) meso-particles in water A; (c) micro-particles in water B; and (d) meso-particles in water B.

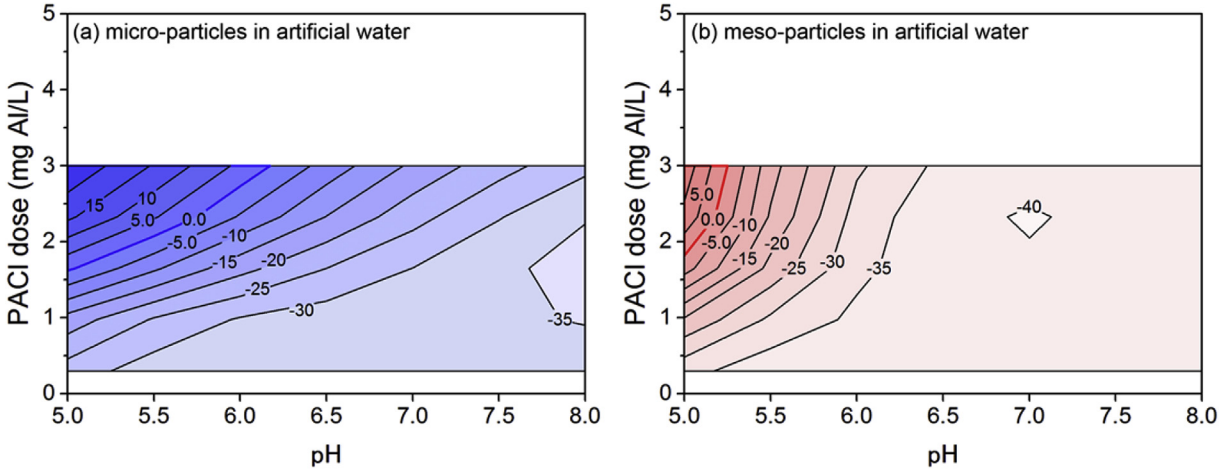

Fig. 3. Effects of pH and PACl dose during coagulation on the zeta potential of (a) micro-particles and (b) meso-particles in artificial water. (The artificial water was made from humic acid sodium salt (Sigma-Aldrich, USA), and filtered through 0.5 μm filter in order to remove undissolved humic acid sodium salt, after which the particle number of meso-particles was about 8.0×10^6 particles/mL, and then used as raw water for jar tests.).

negative charge of the organic materials increases with decreasing pH. The charge of PACl usually increases as pH decreases (Fig. 4). The ZP of the PACl used in this study decreased by 50% from +40 mV to +20 mV as pH increased from 5.0 to 7.0. In dissolvable organic matter, dissociated protons bond with functional groups as pH decreases, so we hypothesized that ZP would increase until it reached the neutralization point. However, there was almost no change in ZP from pH 5.0 to pH 8.0 for the organic matter in water A (Figure S2). Thus, given that the ZP of the PACl was halved at pH 7.0 relative to pH 5.0, the PACl dose required

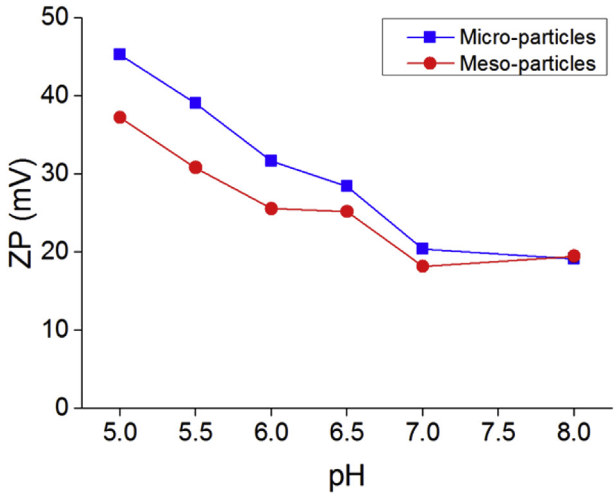

Fig. 4. Effects of pH on zeta potential of pure coagulant PACl. (Micro- and meso-particles were made by the same jar tests processes mentioned in materials and methods after adding 1.0 mg Al/L of PACl into 1 L of pure water.)

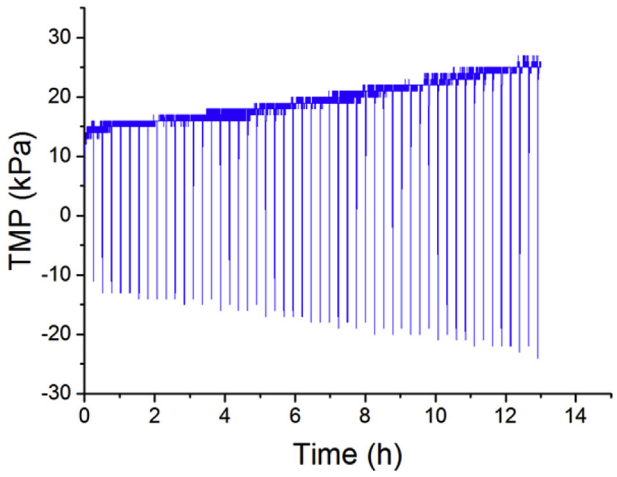

Fig. 5. Change in trans-membrane pressure with time when water A was filtered using a PVDF membrane (PACl dose: 1.0 mg Al/L; pH: 6.5).

to reach the neutralization point at pH 7.0 should be twice that required at pH 5.0. However, since the meso-particles were not neutralized at pH 7.0, even when 1.0 mg Al/L of PACl was added (more than twice the amount required to neutralize them at pH 5.0: 0.4 mg Al/L for water A), we assume that the charge of dissolved organic matter and coagulant does not depend solely on pH or that some other process is affecting the system. The charge neutralization mechanism of meso-particles is a topic for future investigation.

Interestingly, a comparison of Figs. 2 and 3 shows that the PN of meso-particles is extremely high within the low pH range in which they are charge-neutralized. This indicates that although these particles neutralize, coarsening is slow. Since meso-particles are extremely small, Brownian motion is dominant in determining their behavior. Although van der Waals forces normally cause charge-neutralized particles to coagulate or coarsen, we believe that for meso-particles, coarsening tends not to occur under conditions where cross-linking effects are not operating, because Brownian motion causes them to move vigorously.

3.3. Extent of irreversible membrane fouling

Meso-particles are close in size to the membrane pore size, and their lodging in membrane pores is thought to contribute to the process of irreversible membrane fouling. Based on Figs. 2 and 3 we selected six coagulation conditions under which meso-particle characteristics differed substantially, and conducted bench-scale coagulation-membrane filtration experiments using these conditions. With a PVDF membrane, TMP increased as membrane fouling progressed (Fig. 5). Because we removed the cake layers that had accumulated on the membrane surface by means of physical cleaning every 30 min, the increase in TMP shown in Fig. 5 indicates the progression of irreversible membrane fouling. We defined TMP after 13 h as our indicator of the extent of irreversible membrane fouling and used this to summarize the results from the filtration experiments (Fig. 6).

In the tests involving water B, at pH 7.0 and PACl dose of 1.0 mg Al/L, membrane fouling was more rapid than when the source water was filtered directly (Fig. 6). This shows that setting the coagulation conditions appropriately is extremely important in controlling membrane fouling. Although for both types of water membrane fouling was controlled through coagulation under acidic conditions, conditions of best control differed for each water source. For water A these conditions were a pH of 5.5 and a PACl dose of 1.0 mg Al/L, but for water B they were a pH of 6.5–7.0 and a PACl dose of 5.0 mg Al/L. Thus the optimal coagulation conditions for controlling irreversible membrane fouling vary depending on the characteristics of the source water.

For water A, irreversible membrane fouling reduced as the PACl dose increased within the pH range 6.0–8.0, but at pH 5.5 increasing the PACl dose accelerated membrane fouling. Thus increasing the PACl dose alone cannot control irreversible membrane fouling.

Membrane fouling was controlled at low pH levels even though the PN of both meso- and micro-particles increased, for both types of water (Figs. 1 and 6). The fact that the correlation coefficient between the extent of irreversible membrane fouling and PN of both meso- and micro-particles was less than 0.5 (Fig. 7) suggests that quality may be more important than quantity in determining the rate of irreversible membrane fouling.

3.4. Meso-particle characteristics contributing to the rate of irreversible membrane fouling

As the detail correlation types are still unknown, we conducted both linear and quadratic correlation analysis between particle PN or ZP and TMP (Table S2), and used the correlation types with higher corrected R^2 values. As the result, we used quadratic correlation between particle ZP and TMP, rather than linear correlation shown in Fig. 7. From Fig. 8, there was a clear correlation between particle ZP and the extent of irreversible membrane fouling for both water A and water B. For meso-particles this was a second-order correlation, with a correlation coefficient of 0.71 for water A and 0.76 for water B. Irreversible membrane fouling was best controlled, for both types of water, when meso-particle ZP approached zero. The result was similar when a ceramic membrane with a nominal pore size of 0.1 μm was used instead of the PVDF membrane (Fig. 9). This suggests that, regardless of membrane type and source water quality, irreversible membrane fouling can be best controlled by selecting coagulation conditions under which meso-particle ZP approaches zero.

The size of meso-particles is on the same order as that of the membrane pores, and when these particles are retained inside the membrane pores they block passage and cause an increase in

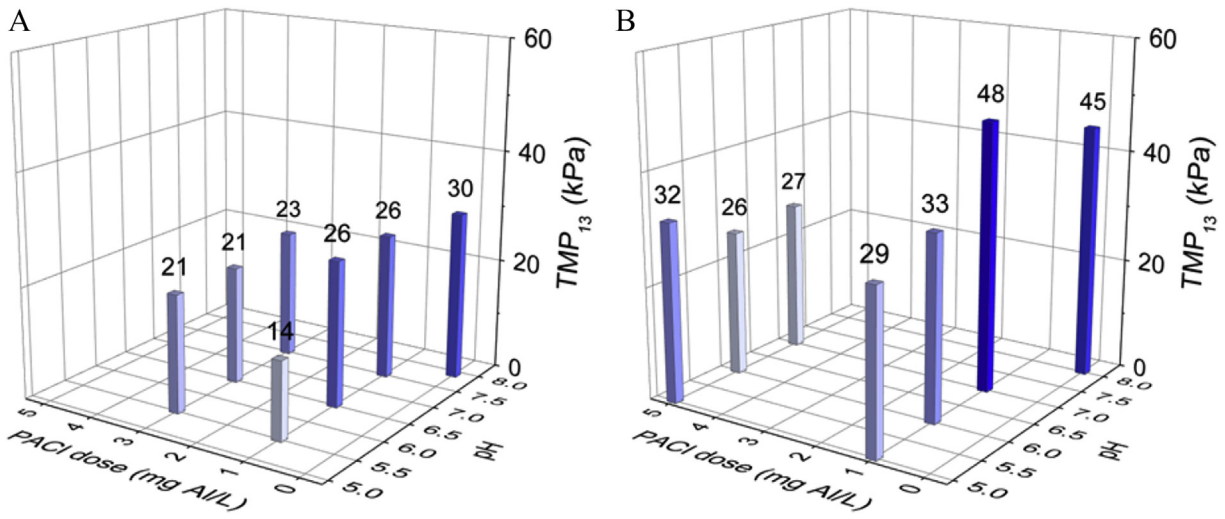

Fig. 6. Effect of coagulation pH and PACl dose on irreversible membrane fouling (left: water A, right: water B). The vertical axis gives trans-membrane pressure values after 13 h (TMP_{13}), as an indicator of the extent of membrane fouling. The numbers above each column represents the TMP_{13} value at each condition.

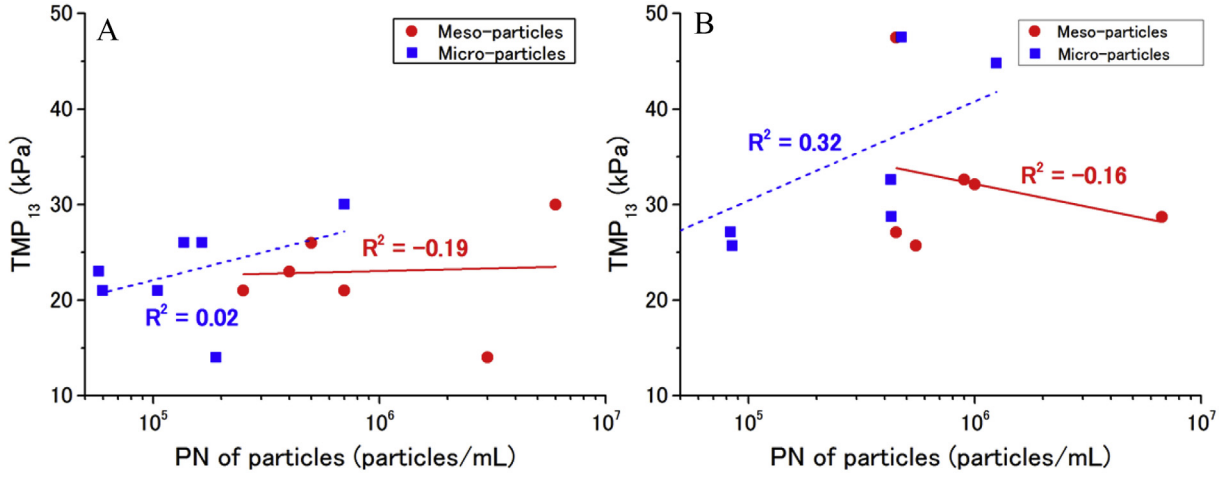

Fig. 7. Relationship between particle number and the extent of irreversible membrane fouling (left: water A, right: water B). The vertical axis gives trans-membrane pressure values after 13 h.

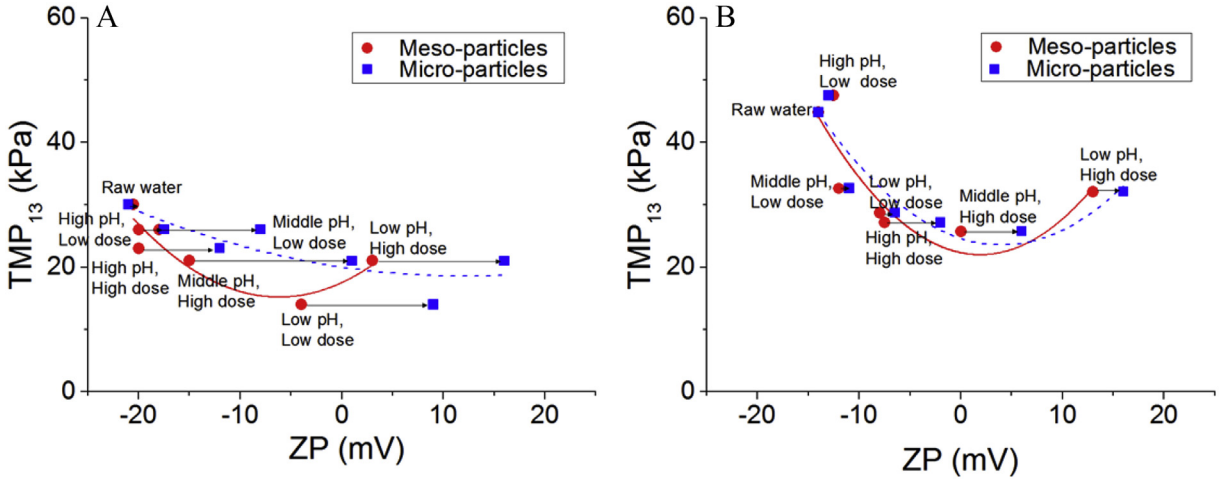

Fig. 8. Relationship between particle zeta potential and the extent of irreversible PVDF membrane fouling (left: water A, right: water B). The vertical axis gives trans-membrane pressure values after 13 h.

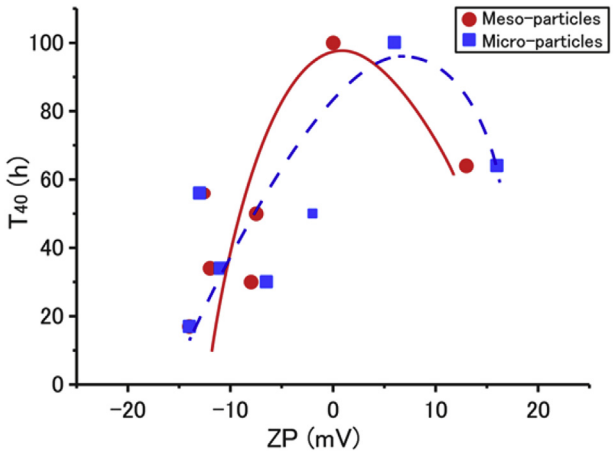

Fig. 9. Relationship between particle zeta potential and extent of irreversible membrane fouling for water B with a ceramic membrane. The vertical axis gives the time at which trans-membrane pressure reached 40 kPa.

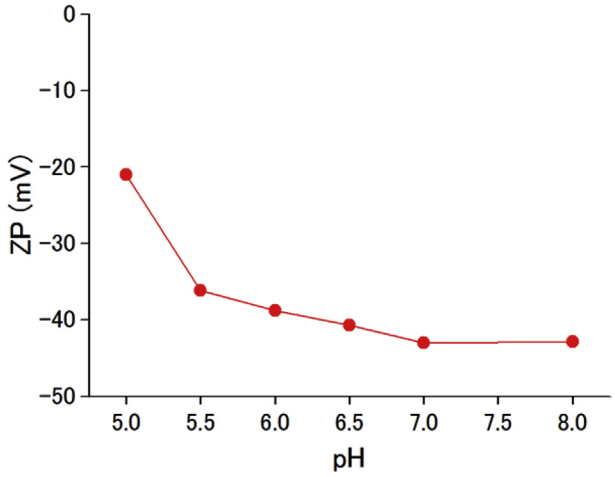

Fig. 10. Effect of pH on the zeta potential of the PVDF powder used to make PVDF membranes.

membrane filtration resistance. For such particles to not be removed by physical cleaning and instead remain in the membrane pores, they must be strongly adsorbed to the membrane surface. At pH 5.0–8.0, the membrane surface is negatively charged (Fig. 10), and if the meso-particles are also negatively charged, they are repelled. However, positively charged dissolved aluminum, calcium, and magnesium are present in the post-coagulation water, and the cross-linking effects due to these cations appear to cause electrostatic adsorption of the negatively charged meso-particles to the membrane surface (Jermann et al., 2007; Li and Elimelech, 2004; Listiarini et al., 2009). In addition, when the meso-particles are positively charged they adhere electrostatically to a negatively charged membrane surface. We suggest that electrostatically adhered meso-particles are difficult to remove with physical cleaning, and thus are responsible for irreversible membrane fouling. We hypothesize therefore that when the meso-particle charge approaches zero, the strength of their electrostatic adhesion to the membrane surface is reduced and they can be removed by physical cleaning.

This indicates that the control of ZP is more important in limiting irreversible membrane fouling than controlling PN of meso-particles and that cations play a crucial role in membrane fouling. Similarly, Jermann et al. (2007) found that humic acid adsorbed to the membrane surface due to the cross-linking effect of calcium, and on this base proposed a mechanism for the process of irreversible membrane fouling. They held that because the hydraulic resistance was greater than what the effect of humic acid could counteract when meso-particles blocked the membrane pores, even a tiny number of meso-particles led to severe fouling.

The relationship between the ZP of micro-particles and the extent of irreversible fouling was weaker than for meso-particles and varied depending on the type of source water (Fig. 8). For water B there was a second-order correlation such that membrane fouling was minimal when ZP was zero for micro-particles, just as for meso-particles. However, for water A irreversible membrane fouling continued to decrease as micro-particle ZP increased above zero. We hypothesize that this is because micro-particles that have accumulated on the membrane surface are easily removed by physical cleaning, resulting in a weaker correlation between micro-particle ZP and extent of irreversible membrane fouling.

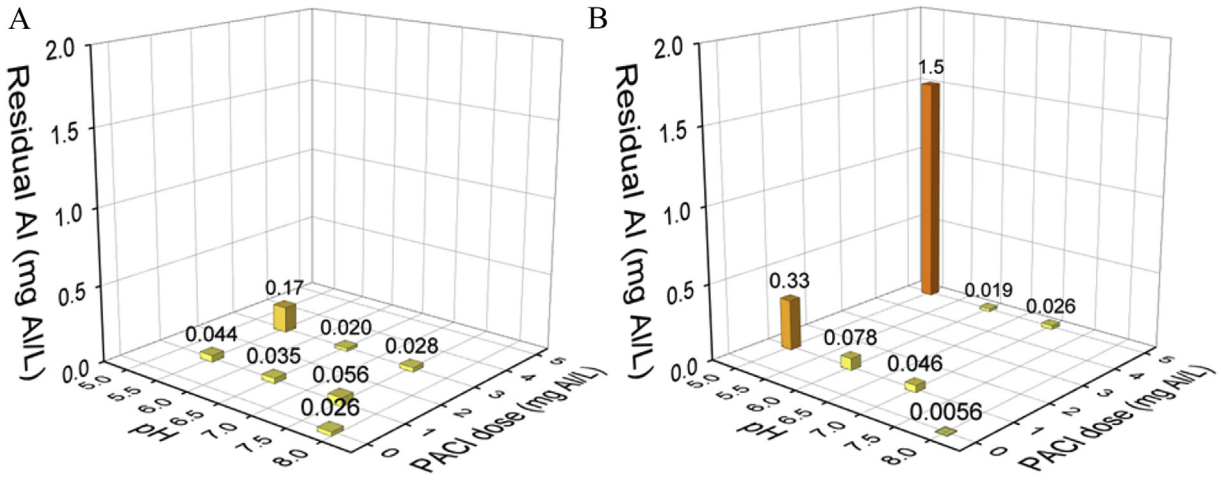

Fig. 11. Effects of coagulation pH and PACl dose on residual aluminum concentration (left: water A, right: water B).

3.5. Determining optimal coagulation conditions by focusing on meso-particle characteristics

Using the relationship between meso-particle ZP and irreversible membrane fouling, we can explore suitable coagulation conditions for coagulation-membrane filtration. Based on existing jar tests, optimal coagulation conditions have been determined based on water quality factors such as concentration of organic matter and turbidity. However, for membrane filtration we must set coagulation conditions according to other factors to control membrane fouling. Based on this study we conclude that membrane fouling can be controlled by measuring the ZP of meso-particles generated following the jar test and selecting conditions such that this value approaches zero. Both types of water used in this study had meso-particle charge neutralization points close to pH 5.5, which means coagulation must take place under more acidic conditions than for typical coagulation. When acidic coagulation took place in water B, coagulation conditions were not optimal because the residual aluminum levels were greater than that of standard tap water (0.2 mg Al/L; Fig. 11).

Furthermore, the acidic water would affect the efficiency of chlorination and pipe corrosion. To escape this situation, in Japan, pH must be returned to circumneutral before disinfection process. However, the cost for pH elevation after filtration would be much higher than the cost saved by prevention of the irreversible membrane fouling at acidic pH. To minimize the total cost for water purification, we believe that we have to achieve the prevention of irreversible membrane fouling under circumneutral pH condition. For this reason, we suggest that in future research it will be necessary to investigate coagulants that bring meso-particle ZP to zero at a circumneutral pH, and also to develop techniques such as pre-oxidation or pre-chlorination for the modification of meso-particle characteristics (e.g., the functional groups on meso-particles). The effects of meso-particles on ultrafiltration membrane fouling are also a topic for future research.

4. Conclusions

In this study, we operationally defined particles into micro- (i.e., >0.5 μm) and meso-particles (i.e., 20 nm–0.5 μm). Physicochemical characteristics including ZP and PN of them were firstly investigated with the use of a new particle tracker combined a high-output violet laser with a microscope. Then the principle factors governing the degree of irreversible membrane fouling were identified based on the repeated membrane filtration experiment using both PVDF and ceramic membranes under various coagulation conditions.

The main results obtained are shown below:

1. Identification of ZP of meso-particles remaining after coagulation was succeeded with the use of ZEECOM equipped with a violet laser.
2. The neutralization points (ZP = 0) were found to be different depending on the size of particle. Under same PACl dose, the neutralization point of meso-particles was lower in pH than that of micro-particles.
3. Under the condition where micro-particles were neutralized, meso-particles tended to remain as negatively charged particles, and it is still difficult to neutralize them even when the PACl dose was increased to 3.0 mg Al/L.
4. Irreversible membrane fouling in both PVDF and ceramic MF membrane was best controlled while meso-particle ZP approached zero.
5. PN of micro- and meso-particles had no relation with irreversible membrane fouling regardless of membrane type and source water.
6. Optimal pre-coagulation condition for the prevention of irreversible membrane fouling, or acidic pH, is not suitable for actual operation, as considering residual aluminum concentration, pipe corrosion, and chlorination efficiency. It is therefore necessary to investigate coagulants or other methods for the appropriate modification of meso-particle characteristics so as to achieve the efficient pre-coagulation from the view point of both water quality and fouling prevention.

Acknowledgment

The authors greatly appreciate the support of Dr. Dabide Yamaguchi from METAWATER Co., Ltd, Japan, who gave advice about the Hybrid Particle Counter (MW-SK121; METAWATER).

Appendix A. Supplementary data

Supplementary data related to this article can be found at http://dx.doi.org/10.1016/j.watres.2016.05.076.

References

Amirtharajah, A., Mills, K.M., 1982. Rapid-mix design for mechanisms of alum coagulation. J. Am. Water Works Assoc. 74 (4), 210–216.
Buffle, J., Wilkinson, K.J., Stoll, S., Filella, M., Zhang, J.W., 1998. A generalized description of aquatic colloidal interactions: the three-colloidal component approach. Environ. Sci. Technol. 32 (19), 2887–2899.
Cho, M.H., Lee, C.H., Lee, S., 2005. Influence of floc structure on membrane permeability in the coagulation-MF process. Water Sci. Technol. 51 (6–7), 143–150.
Choi, K.Y.J., Dempsey, B.A., 2004. In-line coagulation with low-pressure membrane filtration. Water Res. 38 (19), 4271–4281.
Duan, J., Gregory, J., 2003. Coagulation by hydrolysing metal salts. Adv. Colloid Interface Sci. 100–102, 475–502.
Gao, W., Liang, H., Ma, J., Han, M., Chen, Z.L., Han, Z.S., Li, G.B., 2011. Membrane fouling control in ultrafiltration technology for drinking water production: a review. Desalination 272 (1–3), 1–8.
Huang, H., Schwab, K., Jacangelo, J.G., 2009. Pretreatment for low pressure membranes in water treatment: a review. Environ. Sci. Technol. 43 (9), 3011–3019.
Jermann, D., Pronk, W., Meylan, S., Boller, M., 2007. Interplay of different NOM fouling mechanisms during ultrafiltration for drinking water production. Water Res. 41 (8), 1713–1722.
Kimura, K., Hane, Y., Watanabe, Y., Amy, G., Ohkuma, N., 2004. Irreversible membrane fouling during ultrafiltration of surface water. Water Res. 38 (14–15), 3431–3441.
Kimura, K., Maeda, T., Yamamura, H., Watanabe, Y., 2008. Irreversible membrane fouling in microfiltration membranes filtering coagulated surface water. J. Memb. Sci. 320 (1–2), 356–362.
Kimura, K., Tanaka, K., Watanabe, Y., 2014. Microfiltration of different surface waters with/without coagulation: clear correlations between membrane fouling and hydrophilic biopolymers. Water Res. 49, 434–443.
Lead, J.R., De Momi, A., Goula, G., Baker, A., 2006. Fractionation of freshwater colloids and particles by SPLITT: analysis by electron microscopy and 3D excitation-emission matrix fluorescence. Anal. Chem. 78 (11), 3609–3615.
Lebeau, T., Lelievre, C., Buisson, H., Cleret, D., Van de Venter, L.W., Cote, P., 1998. Immersed membrane filtration for the production of drinking water: combination with PAC for NOM and SOCs removal. Desalination 117 (1–3), 219–231.
Lee, J.D., Lee, S.H., Jo, M.H., Park, P.K., Lee, C.H., Kwak, J.W., 2000. Effect of coagulation conditions on membrane filtration characteristics in coagulation-microfiltration process for water treatment. Environ. Sci. Technol. 34 (17), 3780–3788.
Li, M., Jiang, M., Wu, C., 1997. Fluorescence and light-scattering studies on the formation of stable colloidal nanoparticles made of sodium sulfonated polystyrene ionomers. J. Polym. Sci. B Polym. Phys. 35 (10), 1593–1599.
Li, M., Wu, G., Guan, Y., Zhang, X., 2011. Treatment of river water by a hybrid coagulation and ceramic membrane process. Desalination 280 (1–3), 114–119.
Li, Q.L., Elimelech, M., 2004. Organic fouling and chemical cleaning of nanofiltration membranes: measurements and mechanisms. Environ. Sci. Technol. 38 (17), 4683–4693.
Listiarini, K., Chun, W., Sun, D.D., Leckie, J.O., 2009. Fouling mechanism and resistance analyses of systems containing sodium alginate, calcium, alum and their combination in dead-end fouling of nanofiltration membranes. J. Memb. Sci. 344 (1–2), 244–251.
Matilainen, A., Vepsalainen, M., Sillanpaa, M., 2010. Natural organic matter removal

by coagulation during drinking water treatment: a review. Adv. Colloid Interface Sci. 159 (2), 189–197.
Perret, D., Leppard, G.G., Muller, M., Belzile, N., Devitre, R., Buffle, J., 1991. Electron microscopy of aquatic colloids: non-perturbing preparation of specimens in the field. Water Res. 25 (11), 1333–1343.
Singer, P.C., 1994. Control of disinfection by-products in drinking-water. J. Environ. Eng. ASCE 120 (4), 727–744.
Stoller, M., 2009. On the effect of flocculation as pretreatment process and particle size distribution for membrane fouling reduction. Desalination 240 (1–3), 209–217.
Tombacz, E., Filipcsei, G., Szekeres, M., Gingl, Z., 1999. Particle aggregation in complex aquatic systems. Colloids Surf. A Physicochem. Eng. Asp. 151 (1–2), 233–244.
Wiesner, M.R., Clark, M.M., Mallevialle, J., 1989. Membrane filtration of coagulated suspensions. J. Environ. Eng. ASCE 115 (1), 20–40.
Yamamura, H., Okimoto, K., Kimura, K., Watanabe, Y., 2014. Hydrophilic fraction of natural organic matter causing irreversible fouling of microfiltration and ultrafiltration membranes. Water Res. 54, 123–136.